

Quantitative evolution of vacancy-type defects in high-energy ion implanted Si:

Au labeling and the vacancy implanter

R.Kalyanaraman^{a,b}, T.E.Haynes^a, M.Yoon^a, B.C.Larson^a, D.C.Jacobson^b,

H.-J.Gossmann^b, C.S.Rafferty^b

^a Oak Ridge National Laboratory, Solid State Division, Oak Ridge, TN, USA

^b Lucent Technologies, Bell Laboratories, Murray Hill, NJ, USA

In ion implantation related research in Si, the role of interstitial clusters in dopant diffusion is fairly well understood. But there is a relatively poor understanding of vacancy clusters, mainly because of the inadequacy of present techniques to profile and especially to count vacancy defects. Recently two important steps have been taken in the direction of understanding the vacancy-type defects. The first is the demonstration that high-energy ion implantation (HEI) can be used as a *vacancy implanter* to introduce vacancies (V) in Si that are separated from the interstitials (I) by relying on spatial separation of the Frenkel pairs due to the average forward momentum of the recoils. The second is the development of two techniques, Au labeling and cross-section x-ray microbeam diffuse scattering, which permit quantitative measurements of the vacancy-type defect clusters and their depth distribution. In this work, we highlight the Au labeling technique and use the vacancy implanter in conjunction with Au labeling to study the evolution of excess vacancy defects (V_{ex}) created by HEI of Si^+ in Si(100) as a function of dose and temperature. We show that a precise injection of V_{ex} is possible by controlling implanted dose. We also show that the V_{ex} clusters formed by the HEI are

extremely stable and their annihilation is governed by interstitial injection rather than vacancy emission in the temperature range of 800°–900°C.

PACS codes: 61.72.Ji, 61.80.Jh, 82.80.Yc, 85.40.Ry

Keywords: Au labeling, High-energy ion implantation, excess vacancies, vacancy implanter, RBS, Si

Contact Author:

Ramki Kalyanaraman

Lucent Technologies, Bell Labs,

1E-203, 700 Mountain Ave,

Murray Hill, NJ-07974, USA

Email: ramkik@lucent.com

FAX: (908)-582-4228

Introduction

Recently, two techniques, Au labeling [1] and cross-section x-ray diffuse scattering [2], have been used to quantitatively measure the concentration and to profile the vacancy cluster distribution and size of excess vacancies (V_{ex}) generated by HEI into Si [3, 4] respectively. These two new methods present a unique opportunity to study in detail the physics of defect formation from HEI, including specific features like dependence on implanted species, dose, annealing time and temperature, etc. In this work, we briefly describe the Au labeling technique and present some results from a study of the evolution of the excess vacancies under various conditions. Specifically, the possibility of creating a “vacancy implanter,” that rests on the ability to generate specific concentrations of vacancies and controlling the release of free vacancies will be discussed. In this regard, results on the efficiency of V_{ex} production are presented and compared with calculations based on simulations using binary-collision models via the Monte Carlo code TRIM [5]. Finally, the thermal stability of the V_{ex} defects is studied by comparing 2-MeV Si implants in float zone (FZ) and epitaxial (epi) Si substrates to those into specially prepared Si-on-insulator (SOI) substrates having a buried oxide at a depth of 1.5 μm .

Experiment

In this work, p-type FZ Si(100) wafers were used for all studies. Additionally, n-type epi Si(100) and molecular beam epitaxially grown n-type SOI were included for the study on thermal stability of V_{ex} defects. The implants used in this work were carried out using a 1.7 MeV National Electrostatics tandem Pelletron at Bell Laboratories or a similar General Ionex accelerator at Oak Ridge National Laboratory. The 2-MeV Si implants were performed at substrate temperatures of 70°C to prevent amorphization, while the

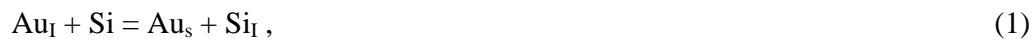
substrates were inclined at an angle of 7° to the implant direction to suppress channeling effects. The Au labeling was carried out by implanting 8×10^{14} - $1 \times 10^{15} \text{ cm}^{-2}$ Au at an energy of 68-keV followed by a 750°C drive-in anneal in flowing Ar (1.5 lpm) at 1 atm. Rutherford backscattering (RBS) analysis of the Au-labeled samples was done using 2.8 or 3.5 MeV $^4\text{He}^{2+}$ at a detector angle of 170° . Transmission electron microscopy (TEM) was carried out in a JEOL-4000 400-keV machine with a point-to-point resolution of 1.6 Å.

Results and Discussion

A. The Au labeling technique

Experimentally, Au labeling is a straightforward technique involving ion implantation and subsequent analysis of Au in Si. A detailed description of this technique has been presented earlier in the work done by Venezia and co-workers [6]. The Si substrate to be profiled is implanted with low-energy Au ions on the front surface with a dose sufficient to saturate the expected V_{ex} concentrations. The Au drive-in anneal is typically carried out for times ranging from 2 hrs to 24 hrs depending upon the concentration of vacancies present. Subsequently, after the Au and vacancy interaction has reached completion, analytical techniques like RBS, secondary ion mass spectroscopy or deep level transient spectroscopy can be used to profile the Au concentration.

The rationale for the use of Au to label vacancy clusters arises from the diffusion mechanism for Au in Si [7]. The kick-out mechanism, by which Au diffuses in Si in a fairly large temperature range [7], results in a Si interstitial being kicked out for every Au atom that becomes substitutional. The reaction can be written as:



where the subscripts denote interstitial (I) and substitutional (S) species respectively. Thus, the formation of substitutional Au, which is effectively immobile because of its low diffusivity [8], is enhanced in the vicinity of interstitial sinks. Using this idea, Venezia and co-workers [6] showed that Au concentrations 3–4 orders of magnitude higher than the solubility could be obtained in the near-surface regions of MeV-implanted Si. This result was clearly shown to be due to the presence of a large excess vacancy concentration because of the MeV implant.

To utilize this technique as an analytical tool, it was necessary to determine the exact relation between the concentration of Au atoms and the number of vacancies. We have recently reported¹ the result of experiments designed to obtain the calibration factor, k , which is the ratio of the number of vacancies annihilated for every Au atom present. The k -factor obtained in our experiments done with 2 MeV, 10^{16} cm^{-2} Si self-implants into FZ Si was $1.2 \pm 20\%$, a value close to that which would be obtained from a pure kick-out mechanism (i.e., 1).

While this approach provides a convenient way to profile and measure vacancy concentrations, there are some caveats relevant to using this technique. For instance, Au gettering at other types of interstitial sinks is well known [9]. Figure 1a shows a typical Au profile measured by RBS using a 3.5 MeV He^{2+} beam. The profile was obtained after Au labeling of a 2 MeV, 10^{16} cm^{-2} self implant in FZ-Si which had a pre-anneal at 815°C for 10 min prior to Au labeling. The projected range (R_p) for this implant is 2 μm . As seen in the figure, besides the Au implant peak at the surface, there is an enhanced Au concentration in the near-surface region (around 1 μm) and also a third peak near 2 μm . While the Au peak around 1 μm (often referred to as the $_R_p$ Au [6]) is due to V_{ex} from

the high-energy implant, the R_p peak is because of Au gettering to the end-of-range (EOR) damage, which is interstitial type. These defects are readily apparent in the micrograph, Fig. 1b.

Another important consideration is the state of the vacancy cluster defects. It has been reported [10] that many metals including Au are chemisorbed on the internal surfaces of cavities and voids formed by H [11] or He [12] radiation in Si. These cavities are extremely large in size (10–100 nm) and are easily observable by electron microscopy. For such conditions, the k-factor will be much larger than 1, as determined by the surface-to-volume ratio of the voids. In our studies we have not observed the formation of large voids or cavities, and the fact that k is so close to unity suggests that the Au trapping for these smaller vacancy clusters must be space-filling. Figure 1b shows a cross-section transmission electron micrograph of a 2-MeV, $1 \times 10^{16} \text{ cm}^{-2}$ self-implanted FZ-Si annealed at 815°C for 10 min, showing only the interstitial-type damage at the EOR extending from $\sim 1.5 \mu\text{m}$ and deeper. High-resolution studies of this sample did not reveal any vacancy clusters indicating that either the cluster sizes are extremely small or the concentration of any large clusters is very low. Since this is the highest dose studied, it is presumed that large clusters do not form in the lower dose samples studied. Using this technique and the determined k-factor of 1.2, we have subsequently carried out a quantitative study of the dose and temperature dependence of V_{ex} produced by 2-MeV self-implants in Si.

B. Vacancy implanter

The spatial separation of the Frenkel-pairs produced during damage by ion irradiation in Si [3,4] provides the opportunity to introduce controlled amounts of vacancies near the surface. The concept of a “vacancy implanter” refers to a set of experimental steps that permit injection of controlled amounts of vacancies and release free vacancies to generate large supersaturations. To achieve this, we first used the Au labeling technique to quantitatively measure the injected vacancy concentration via HEI in Si, following which we studied the behavior of the injected V_{ex} concentration as a function of annealing temperature. In Fig. 2a, the V_{ex} profiles obtained via the Au labeling technique as a function of the implanted dose (Φ) is shown. The Au labeling was carried out in as-implanted samples to maximize the concentration of V_{ex} observed. The concentration scale in this figure was obtained by multiplying the Au concentration scale obtained via RBS by the k-factor of 1.2, giving directly the V_{ex} concentration. Figure 2b plots the integrated V_{ex} concentration (in the depth region of 0.6–1.6 μm) as a function of Φ for the 2 MeV self-implants in the dose range of 2×10^{15} to $1 \times 10^{16} \text{ cm}^{-2}$. Clearly, in this dose range the V_{ex} increases linearly with Φ . Also shown in the figure is the V_{ex} for the same depth window obtained from simulation using the TRIM code version SRIM 2000 [5] and a rapid approximation technique detailed elsewhere [13]. The most striking difference is in the efficiency of V_{ex} production with Φ , which is larger for the simulation than that for the experiment (i.e., 0.16 vs. 0.05 vacancies per implanted Si ion). While the exact reasons are still unclear, the simulation only accounts for local recombination of V-I and does not take into account various recombination sites like the EOR and the surface. As we show below, the temperature dependence of the V_{ex} concentration is determined

by the injection of interstitials from the EOR. It is therefore conceivable that the lower efficiency observed by the experiment can partly be attributed to recombination of V_{ex} with interstitials from the EOR.

The second aspect of the vacancy implanter is to provide large supersaturations of free vacancies. In this regard, the thermal stability of the V_{ex} formed by a 2 MeV, $6 \times 10^{15} \text{ cm}^{-2}$ self-implant was studied. FZ, epi, and SOI substrates were chosen to study the thermal evolution of V_{ex} . The thickness of the Si over the buried oxide layer was $1.5 \mu\text{m}$, while the buried oxide layer was $0.2\text{-}\mu\text{m}$ -thick. Since the 2-MeV Si implant has a R_p of $2 \mu\text{m}$, the EOR of the implant was located behind the buried oxide layer. Also, the oxide is known to be a barrier against interstitial diffusion [14] and so the SOI structure inhibits any interaction between the EOR interstitials and V_{ex} . Following the implant, the samples were annealed between $800^\circ\text{--}900^\circ\text{C}$ for 10 min in flowing Ar (1.5 lpm) at 1 atm. Subsequently, the samples were labeled with Au until saturation to determine the V_{ex} concentration. Figure 3a shows the typical V_{ex} profiles for the FZ, epi, and SOI samples after annealing at 875°C . The position of the buried oxide of the SOI is also marked. The major difference in the profiles appears to be in the concentration of V_{ex} in the region closer to the R_p , (i.e., between $1\text{--}1.6 \mu\text{m}$). The SOI sample clearly has a higher concentration than either the FZ or epi samples in this region. In Fig. 3b, the integrated V_{ex} concentration in the depth window of $0.5\text{--}1.5 \mu\text{m}$ is shown plotted as a function of T. Clearly, the V_{ex} in the FZ and epi substrates decreases rapidly as compared with the SOI. This is a clear indication that V_{ex} annihilation is controlled by interstitial injection and not by evaporation. This observation is consistent with the high stability for V_{ex} observed by Venezia [15] and also highlights the difficulty of obtaining large supersaturations of free

vacancies via this technique. In other words, following the implantation in bulk Si the free V_{ex} combine to form stable clusters whose annihilation rate is subsequently controlled by the injection of interstitials from the EOR.

Conclusion

We have reported on the development of the Au labeling technique for the measurement of the concentration of V_{ex} defects from high-energy ion implanted Si. This technique is a convenient way to measure the concentration of V_{ex} with sensitivity determined by the ability to detect Au in Si. Care must be taken in using the calibration factor, k , to determine V_{ex} concentrations as other interstitial sinks, as well as cavities and voids can change this number. Results reported here indicate that while precise vacancy injection is possible, the control of the free-vacancy supersaturation is limited due to the high thermal stability of the V_{ex} clusters. This stability was clearly observed by comparing the behavior of V_{ex} in FZ and epi-Si to SOI, where the buried oxide to prevented interaction between the EOR interstitials and V_{ex} .

Acknowledgments

R.K. would like to thank Cliff King for growing the thick silicon overlayer on SOI and George Celler for providing the SOI. A portion of this research was performed at Oak Ridge National Laboratory and sponsored by the U.S. Department of Energy, Office of Science, Laboratory Technology Research Division and the Division of Materials Sciences under contract DE-AC05-00OR22725 with UT-Batelle, LLC.

References

-
- [1] R.Kalyanaraman, T.E.Haynes, V.C.Venezia, D.C.Jacobson, H.-J.Gossmann, and C.S.Rafferty, *Appl. Phys. Lett.* **76**, 3379 (2000).
- [2] M.Yoon, B.C.Larson, J.Z.Tischler, T.E.Haynes, J.-S.Chung, G.E.Ice, and P.Zschack, *Appl. Phys. Lett.* **75**, 2791 (1999).
- [3] O.W.Holland, L.Xie, B.Nielsen, and D.S.Zhou, *J. Elec. Mat.* **25**, 99 (1996).
- [4] A.M.Mazzone, *Phys. Stat. Sol. (a)* **95**, 149 (1986).
- [5] J.F.Ziegler, J.P.Bierszack, and U.Littmark, *The Stopping and Ranges of Ions in Solids* (Pergamon, New York, 1985).
- [6] V.C.Venezia, D.J.Eaglesham, T.E.Haynes, A.Agarwal, D.C.Jacobson, H.-J.Gossmann, and F.H.Baumann, *Appl. Phys. Lett.* **73**, 2980, (1998).
- [7] U.Gösele, W.Frank, and A.Seeger, *Appl. Phys.* **23**, 361 (1980).
- [8] K.Graff, *Metal impurities in Si-device fabrication*, (Springer-verlag, New York, 1995).
- [9] T.E.Seidel, R.L.Meek, and A.G.Cullis, *J. Appl. Phys.* **46**, 600 (1975); H.Wong, N.Cheung, and P.K.Chu, *Appl. Phys. Lett.* **52**, 889 (1998).
- [10] D.M.Follstaedt, S.M.Myers, G.A.Petersen, J.W.Medernach, *J. Elec. Mat.* **25**, 151 (1996).
- [11] J.Wong-leung, C.E.Ascheron, M.Petravic, R.G.Elliman, and J.S.Williams, *Appl. Phys. Lett.* **66**, 1231 (1995).
- [12] S.M.Myers, D.M.Bishop, D.M.Follstaedt, H.J.Stein, and W.R.Wampler, *Mater. Res. Soc. Symp. Proc.* **283**, 549 (1993).

[13] R.Kalyanaraman, T.E.Haynes, D.C.Jacobson, H.-J.Gossmann, and C.S.Rafferty, to appear in Mater. Res. Soc. Symp. Proc. **610**, (2000).

[14] D.Tsoukalas, C.Tsamis, and J.Stoemenos, App. Phys. Lett. **63**, 3167 (1993).

[15] V.C.Venezia, in Ph.D. Thesis, "Creation and Evolution of the vacancy supersaturation in MeV implanted Si," University of North Texas, Denton, Texas, May (1999).

Figure Captions:

Fig 1 (a) Au labeling profile of a 2-MeV, $1 \times 10^{16} \text{ cm}^{-2}$ self-implanted Si using 3.5-MeV $^4\text{He}^{2+}$ beam. The surface, vacancy (around $1 \mu\text{m}$) and interstitial (around $2 \mu\text{m}$) peaks are clearly seen. (b) Cross-section TEM micrograph of the above sample before Au labeling showing only interstitial defects around $2 \mu\text{m}$. The sample was annealed at 815°C , 10 min prior to Au labeling.

Fig 2 (a) Au profiles for 2-MeV Si implants as a function of dose. (b) The integrated V_{ex} concentration ($0.6\text{--}1.6 \mu\text{m}$) as a function of dose for experiment and simulation.

Fig 3 (a) Au profiles for 2-MeV, $6 \times 10^{15} \text{ cm}^{-2}$ Si implanted into FZ, epi, and SOI substrates after anneal at 875°C for 10 min. The $0.2\text{-}\mu\text{m}$ thick buried oxide layer at a depth of $1.5 \mu\text{m}$ is also shown. (b) Integrated V_{ex} ($0.5\text{--}1.5 \mu\text{m}$) plotted as a function of annealing temperature for the three substrates. The SOI clearly shows that the thermal behavior of the V_{ex} is determined by interstitials from the end-of-range damage.

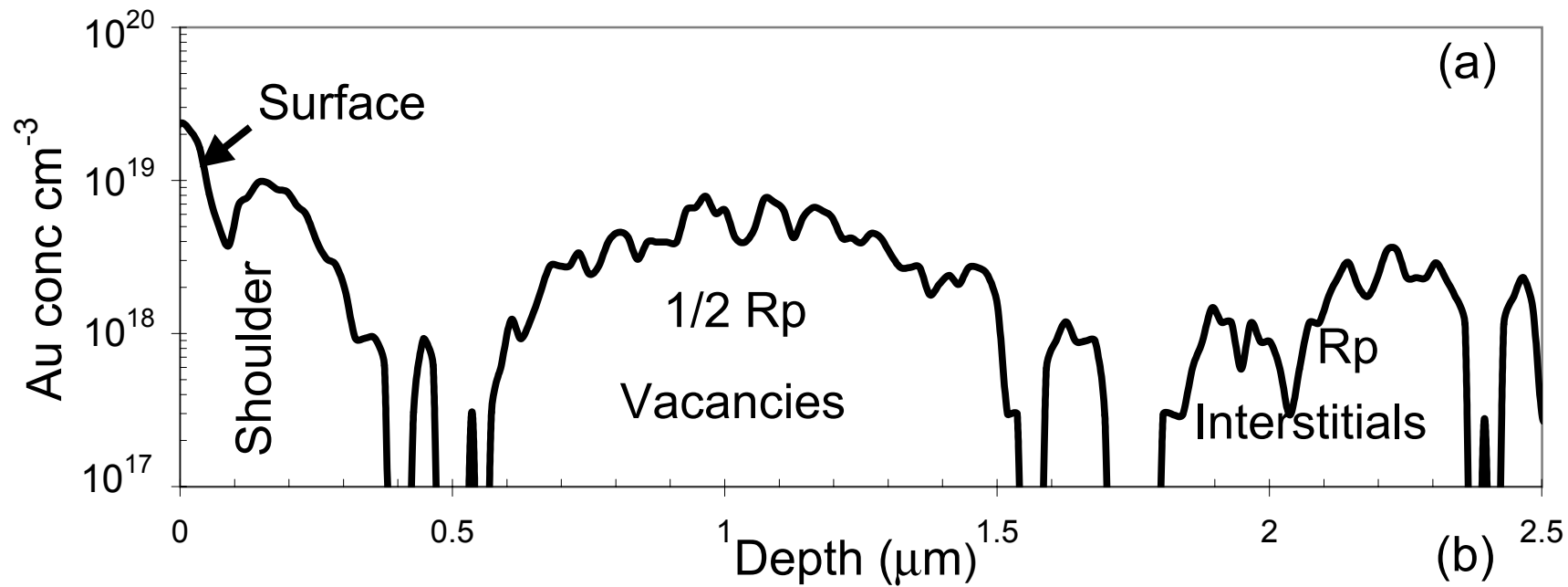


Fig 1

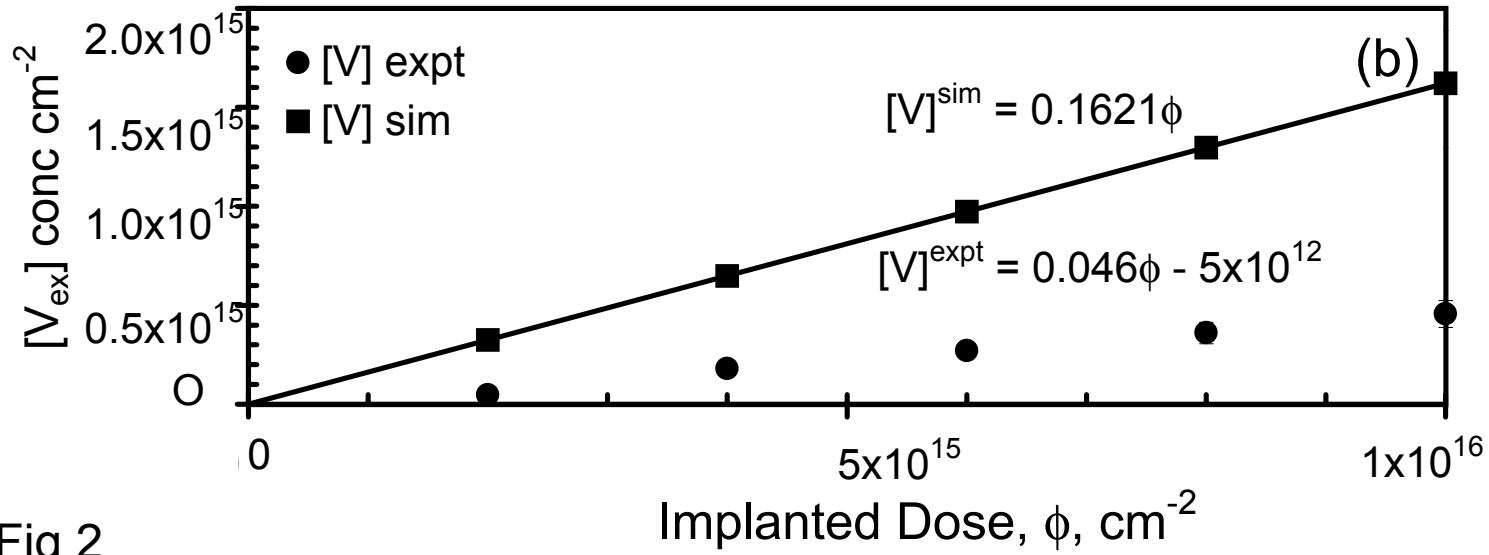
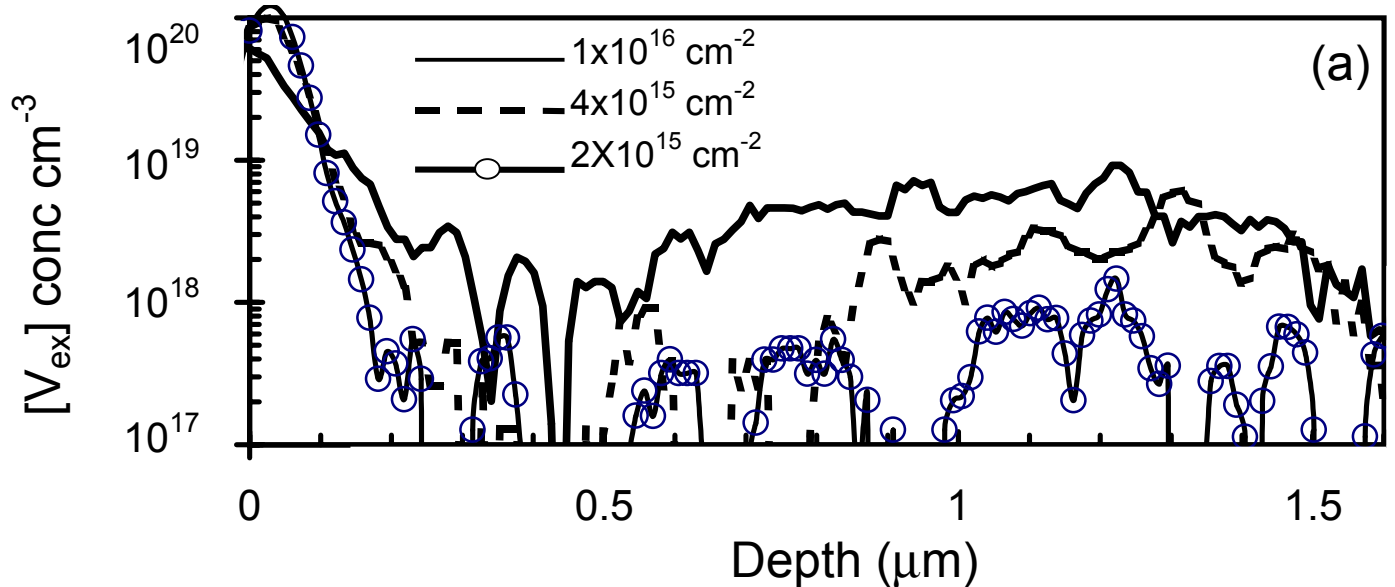


Fig 2

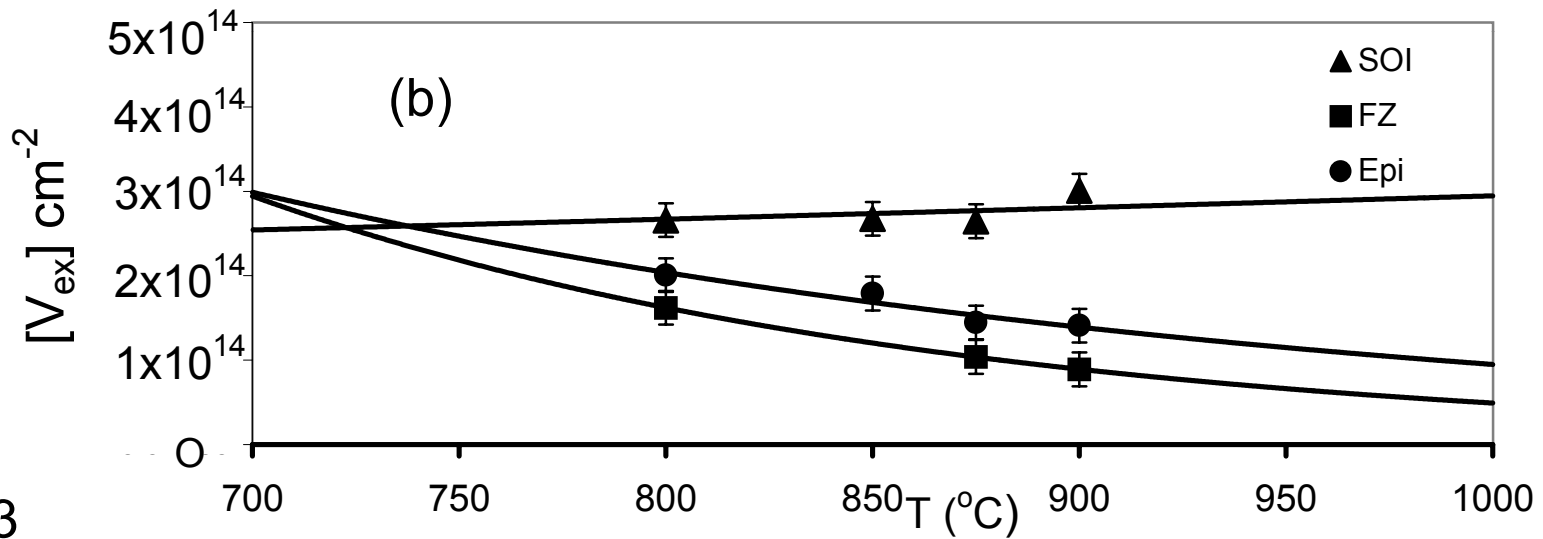
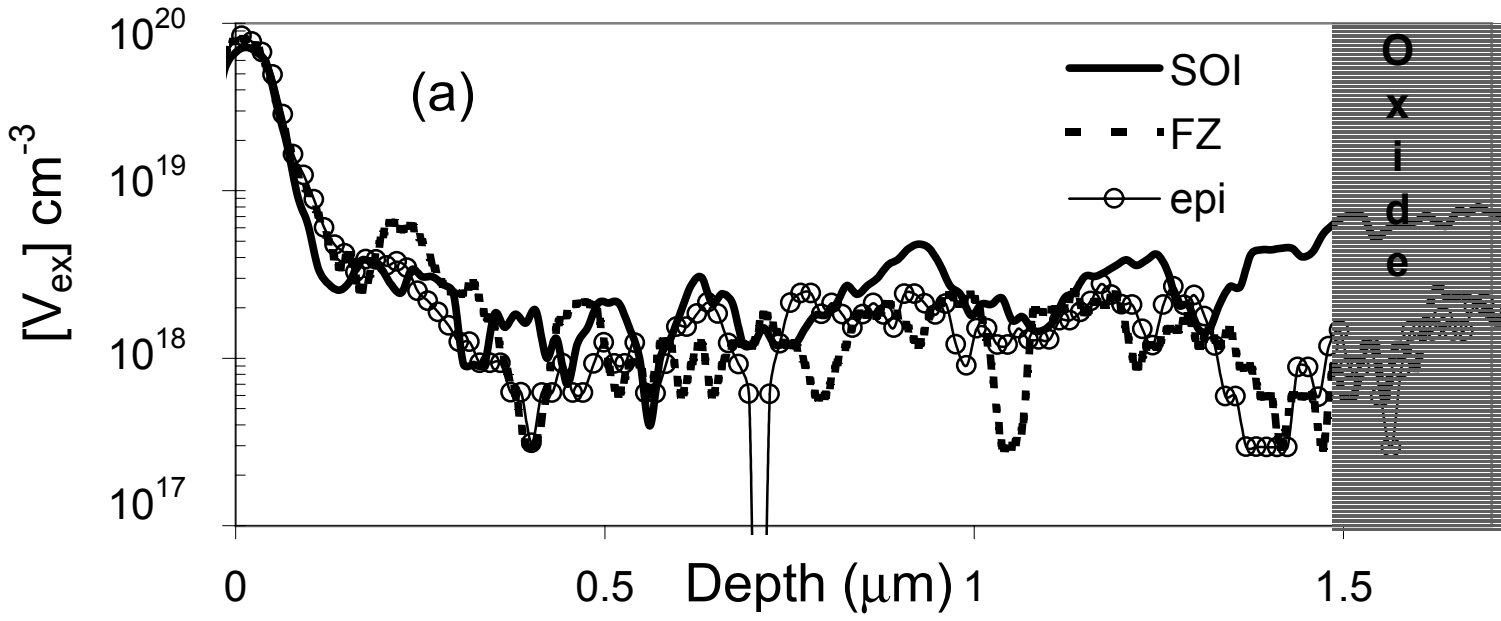


Fig 3